

Aurora A Kinase Regulates Mammary Epithelial Cell Fate by Determining Mitotic Spindle Orientation in a Notch-Dependent Manner

Joseph L. Regan,¹ Tony Sourisseau,^{1,5} Kelly Soady,¹ Howard Kendrick,^{1,6} Afshan McCarthy,² Chan Tang,^{1,7} Keith Brennan,³ Spiros Linardopoulos,^{1,4} Donald E. White,¹ and Matthew J. Smalley^{1,6,*}

¹Division of Breast Cancer Research, Breakthrough Breast Cancer Research Centre, The Institute of Cancer Research, 237 Fulham Road, London SW3 6JB, UK

²Oncogene Team, Division of Cancer Biology, The Institute of Cancer Research, 237 Fulham Road, London SW3 6JB, UK

³Wellcome Trust Centre for Cell Matrix Research, Faculty of Life Sciences, University of Manchester, Manchester, Oxford Road, Manchester M13 9PT, UK

⁴Cancer Research UK, Cancer Therapeutics Unit, The Institute of Cancer Research, 15 Cotswold Road, Sutton SM2 5NG, UK

⁵Present address: Inserm Unit 981, Institut Gustave Roussy, Villejuif 94800, France

⁶Present address: European Cancer Stem Cell Research Institute and Cardiff School of Biosciences, Cardiff University, Hadyn Ellis Building, Maindy Road, Cardiff CF24 4HQ, UK

⁷Present address: Crucell Vaccine Institute, Archimedesweg 4, 2333 CN Leiden, The Netherlands

*Correspondence: smalleymj@cardiff.ac.uk

<http://dx.doi.org/10.1016/j.celrep.2013.05.044>

This is an open-access article distributed under the terms of the Creative Commons Attribution-NonCommercial-No Derivative Works License, which permits non-commercial use, distribution, and reproduction in any medium, provided the original author and source are credited.

SUMMARY

Cell fate determination in the progeny of mammary epithelial stem/progenitor cells remains poorly understood. Here, we have examined the role of the mitotic kinase Aurora A (AURKA) in regulating the balance between basal and luminal mammary lineages. We find that AURKA is highly expressed in basal stem cells and, to a lesser extent, in luminal progenitors. Wild-type AURKA expression promoted luminal cell fate, but expression of an S155R mutant reduced proliferation, promoted basal fate, and inhibited serial transplantation. The mechanism involved regulation of mitotic spindle orientation by AURKA and the positioning of daughter cells after division. Remarkably, this was NOTCH dependent, as NOTCH inhibitor blocked the effect of wild-type AURKA expression on spindle orientation and instead mimicked the effect of the S155R mutant. These findings directly link AURKA, NOTCH signaling, and mitotic spindle orientation and suggest a mechanism for regulating the balance between luminal and basal lineages in the mammary gland.

INTRODUCTION

The mammary epithelium consists of two main lineages: luminal epithelial cells, and basal myoepithelial cells. The former line the ducts and form the milk-secreting cells of the alveoli, whereas the latter are contractile and squeeze milk along the ducts during lactation. The luminal cells are themselves either estrogen receptor α positive (ER+) or negative (ER-). ER+ cells are hormone

sensing and transduce systemic hormonal signals into localized control of epithelial function through paracrine interactions. The ER- cells include the milk secretory cells (Regan et al., 2012; Richert et al., 2000).

The myoepithelial, hormone-sensing ER+ and secretory ER- cells are considered to be the main differentiated populations in the mammary epithelium. Stem and progenitor cells have also been identified by functional assays and/or lineage tracing. Functional assays (the ability of stem and progenitor cells to transplant *in vivo* and proliferate *in vitro*, respectively) support a model in which stem cells are found in the basal layer, together with the myoepithelial cells, whereas cells with progenitor function are highly enriched in the luminal cell layer (Shackleton et al., 2006; Sleeman et al., 2007; Taddei et al., 2008; Stingl et al., 2006). Luminal progenitors are mainly ER-, but a small subfraction of ER+ cells also have progenitor features (Regan et al., 2012; Beleut et al., 2010). During early mammary development and also when purified stem and progenitor subpopulations are transplanted, the basal stem cells have the potential to generate all the other cell types in the mammary epithelium with high efficiency (Shackleton et al., 2006; Sleeman et al., 2007; Stingl et al., 2006; Regan et al., 2012). In contrast, *in situ* lineage analysis of normal adult tissue suggests that in the resting postpubertal gland, the basal and luminal cell layers are maintained as separate lineages (Van Keymeulen et al., 2011; van Amerongen et al., 2012). These findings argue that the myoepithelial and luminal lineages are maintained by separate stem/progenitor populations in the adult gland. However, at some adult stages, including alveologenesis, basal stem cells may contribute to generating the luminal layer (van Amerongen et al., 2012). Furthermore, analysis of cap cells, the outermost cell layer of the specialized growth structure that drives ductal growth during puberty (the terminal end buds or TEBs), has suggested that they can contribute to both the myoepithelial and

luminal lineages (Srinivasan et al., 2003; Williams and Daniel, 1983).

Stem cells are defined by their potential to self-renew and to generate a defined set of differentiated progeny (Lechler and Fuchs, 2005). Stem cell homeostasis involves asymmetric divisions, with one daughter cell differentiating and one self-renewing. For stem cell expansion, cell divisions must be symmetric, with both daughters of the dividing cell assuming stem cell fate. The balance between asymmetric and symmetric division is regulated by both intrinsic and extrinsic mechanisms (Horvitz and Herskowitz, 1992). The former depends on the partitioning of determinants prior to mitosis that promote the stem cell fate, with equal distribution of the determinants between daughter cells leading to stem cell expansion, and unequal distribution to the daughters adopting different fates and stem cell homeostasis (Betschinger and Knoblich, 2004). In contrast, extrinsic mechanisms depend on interactions between stem cells and their daughters and the microenvironment or niche (Li and Xie, 2005). In this case, the position of postdivision daughter cells, in or out of the niche, will determine whether they assume stem cell identity or an alternative fate.

Aurora A (AURKA) is a centrosomal and mitotic spindle-associated kinase that coordinates mitotic events, regulates centrosome maturation and bipolar spindle formation, and may be involved in both stem cell fate control mechanisms. In *Drosophila*, AURKA can establish polarity during asymmetric cell division in a BORA-dependent manner (Hutterer et al., 2006), thus determining the position of daughter cells with respect to the microenvironment. AURKA also regulates the partitioning of NUMB, an important cell fate determinant and negative regulator of NOTCH signaling, within the cytoplasm prior to division (Cayouette and Raff, 2002).

Here, we examine the role of AURKA as a regulator of mammary stem/progenitor cell behavior and cell fate determination. We show that AURKA can regulate the balance between the luminal and basal myoepithelial cell lineages by regulating the orientation of the mitotic spindle and thus the location of the post-mitotic daughter cells. This mechanism is directly dependent on NOTCH signaling but is independent of NUMB localization. Rather, it requires activity of the NOTCH signaling pathway itself. These findings directly link AURKA, NOTCH signaling, and mitotic spindle orientation and suggest a mechanism for regulating the balance between mammary cell lineages.

RESULTS

AurkA Is Highly Expressed in Mammary Epithelial Stem and Progenitor Cells

To determine the pattern of *AurkA* expression in stem, progenitor, and differentiated mammary epithelial cells, these subpopulations were freshly isolated by flow cytometry from 10-week-old virgin mice (Figures 1A, 1B, S1, and S2A) according to previously defined markers (Regan et al., 2012) and *AurkA* gene expression levels determined by quantitative real-time reverse-transcription PCR. *AurkA* was expressed at significantly higher levels in the stem cells ($CD45^- CD24^{+/\text{Low}} Sca-1^- CD49f^{\text{High}}$ c-Kit $^-$) and luminal ER $-$ progenitors ($CD45^- CD24^{+/\text{High}} Sca-1^- c\text{-Kit}^+$) compared to both the myoepithelial ($CD45^- CD24^{+/\text{Low}} Sca-1^-$

$CD49f^{\text{Low}}$ c-Kit $^-$) and differentiated luminal ER $+$ ($CD45^- CD24^{+/\text{High}} Sca-1^+ c\text{-Kit}^-$) populations. Furthermore, expression of *AurkA* was significantly ($p < 0.05$) (Cumming et al., 2007) higher in the stem cells compared to the progenitors (Figure 1C). *AurkA* expression correlated with expression of *Cyclin B* (a G2/M cyclin) but not *Cyclin D1* (a G1 cyclin), consistent with its role in mitosis (Figure 1C).

To test comparative AURKA protein expression in the four populations, fresh samples were isolated by flow cytometry, fixed, stained for AURKA expression, and then analyzed again by flow cytometry in five independent experiments. Percentages of AURKA-positive cells across the experiments varied quite widely; however, in all experiments, the stem cell population contained the highest percentage of AURKA positive cells (Figure S2).

S155R AURKA Reduces Proliferation of Mammary Epithelial Cells in Monolayer Culture and Promotes Their Differentiation into Myoepithelial Cells

To investigate the function of AURKA in mammary epithelial cells in vitro, freshly harvested primary mammary epithelial cells were transduced with lentiviruses driving expression of GFP only (empty vector control; EV), wild-type AURKA plus GFP (WT), or a mutant form of AURKA plus GFP (S155R) and placed in monolayer culture at identical plating densities. S155R cannot bind to its regulator TPX2 nor can it be targeted by PP1 phosphatase. As a result, it forms a constitutively, but weakly, active protein that associates only with the centrosomes of mitotic cells and not the mitotic spindles (Bibby et al., 2009). The TPX2-AURKA interaction is required to form mitotic spindles of the correct length (Bird and Hyman, 2008).

To confirm that the expressed proteins localized as expected, epithelial cell colonies were fixed after 10 days and stained for AURKA, TPX2, and EG5, which associates with the AURKA-TPX2 complex on mitotic spindles (Ma et al., 2011) (Figure S3). As expected, TPX2 could be seen decorating the mitotic spindles of dividing cells in all cultures. AURKA and EG5 also decorated the mitotic spindles in EV- and WT-transduced cultures. However, in S155R-transduced cells, both AURKA and EG5 were restricted to the centrosomal region, demonstrating that their localization to the mitotic spindle was dependent on the TPX2-AURKA interaction.

Next, transduced colonies were fixed and stained for the basal lineage marker keratin 14 (K14) and the luminal lineage marker keratin 18 (K18) (Figure 2A). For each sample, the mean number of GFP $^+$ -transduced cells per field of view was determined (Figure 2B). There was no significant difference in the number of GFP $^+$ cells in WT cultures compared to EV-transduced cells ($\text{mean} \pm \text{SD}$, 83.22 ± 2.75 versus 76.4 ± 8.5 GFP $^+$ cells per field, respectively). However, the mean number of GFP $^+$ S155R cells was significantly lower (46.42 ± 11.83 GFP $^+$ cells per field; $p < 0.05$ t test versus EV and WT-transduced cells).

When primary mouse mammary cells are isolated and grown in short-term culture under standard conditions, the majority of cells that proliferate are derived from the luminal ER $-$ progenitor population (Sleeman et al., 2007; Regan et al., 2012). In monolayer culture, these luminal cells, which express low levels of K14 in vivo (Regan et al., 2012), upregulate K14 expression and acquire a K14 $^+$ K18 $^+$ phenotype (Sleeman et al., 2007). To examine whether

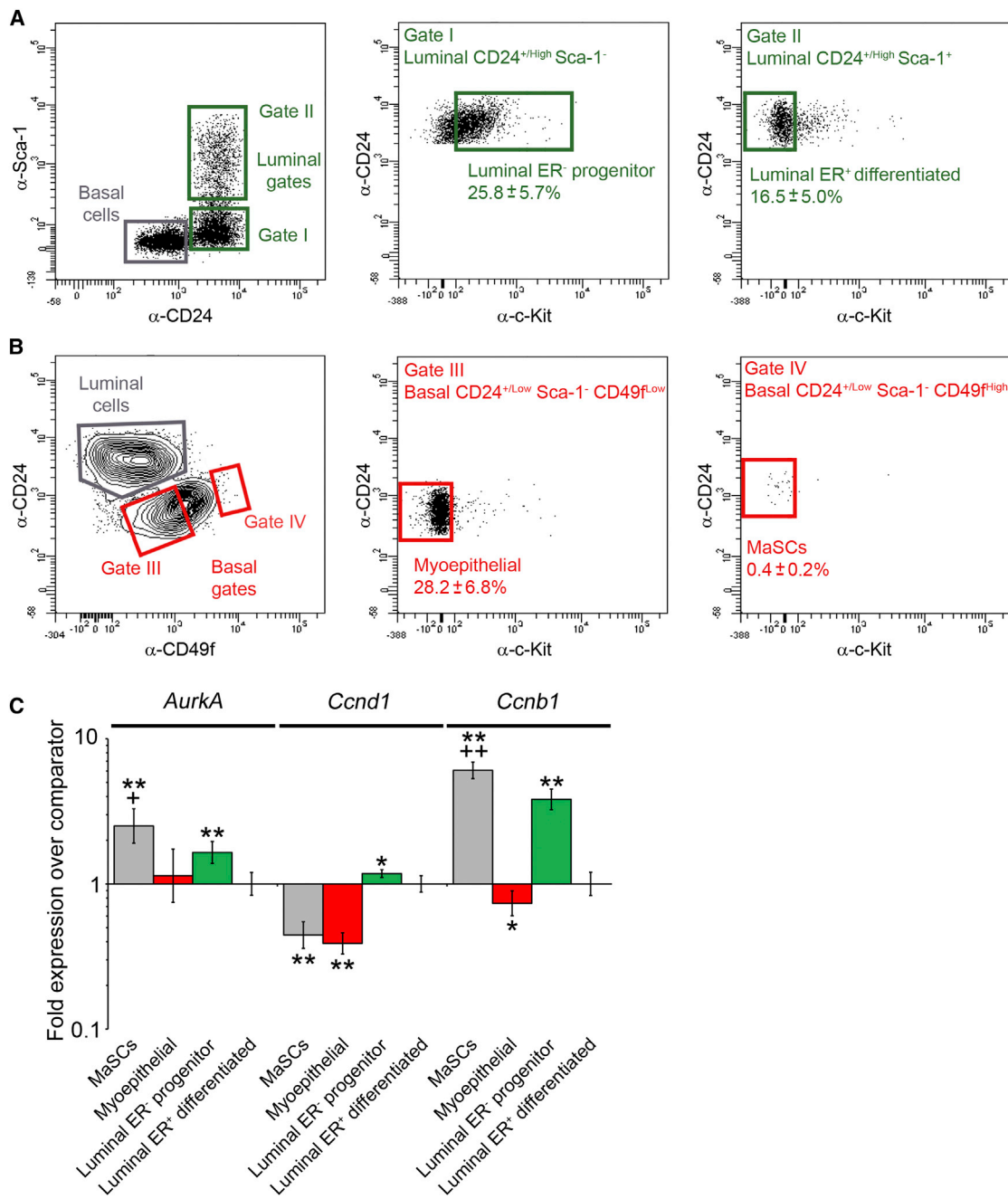


Figure 1. *AurkA* Is Expressed in Mammary Epithelial Stem Cells

(A) Isolation of the luminal ER- and luminal ER+ cell populations by flow cytometry on the basis of CD24 and Sca-1 expression followed by c-Kit as previously described (Regan et al., 2012).

(B) Isolation of basal myoepithelial and mammary stem cells (MaSCs), from the same sort data as in (A), on the basis of CD24 and CD49f expression as previously described (Regan et al., 2012). Only epithelial cell data are shown. See Figure S1 for the full-gating cascade and Figure S2A for postsort purity analysis. The proportion of the total mammary epithelium formed by each of the gated sorted regions is indicated (mean ± SD; n = 4 independent tissue preparations).

(C) Expression of *AurkA*, *Ccnd1*, and *Ccnb1* in mouse mammary subpopulations determined by quantitative real-time reverse-transcription PCR analysis. Data are expressed as mean fold expression (±95% confidence intervals) over comparator population (the luminal ER+ differentiated cells) in three independent isolates of each cell population. Statistical significance was determined according to Cumming et al. (2007). *p < 0.05 relative to comparator; **p < 0.01 relative to comparator; +p < 0.05 in MaSCs relative to progenitors; ++p < 0.01 in MaSCs relative to progenitors. See Figures S2B and S2C for analysis of AURKA protein staining in sorted subpopulations.

See also Figures S1 and S2.

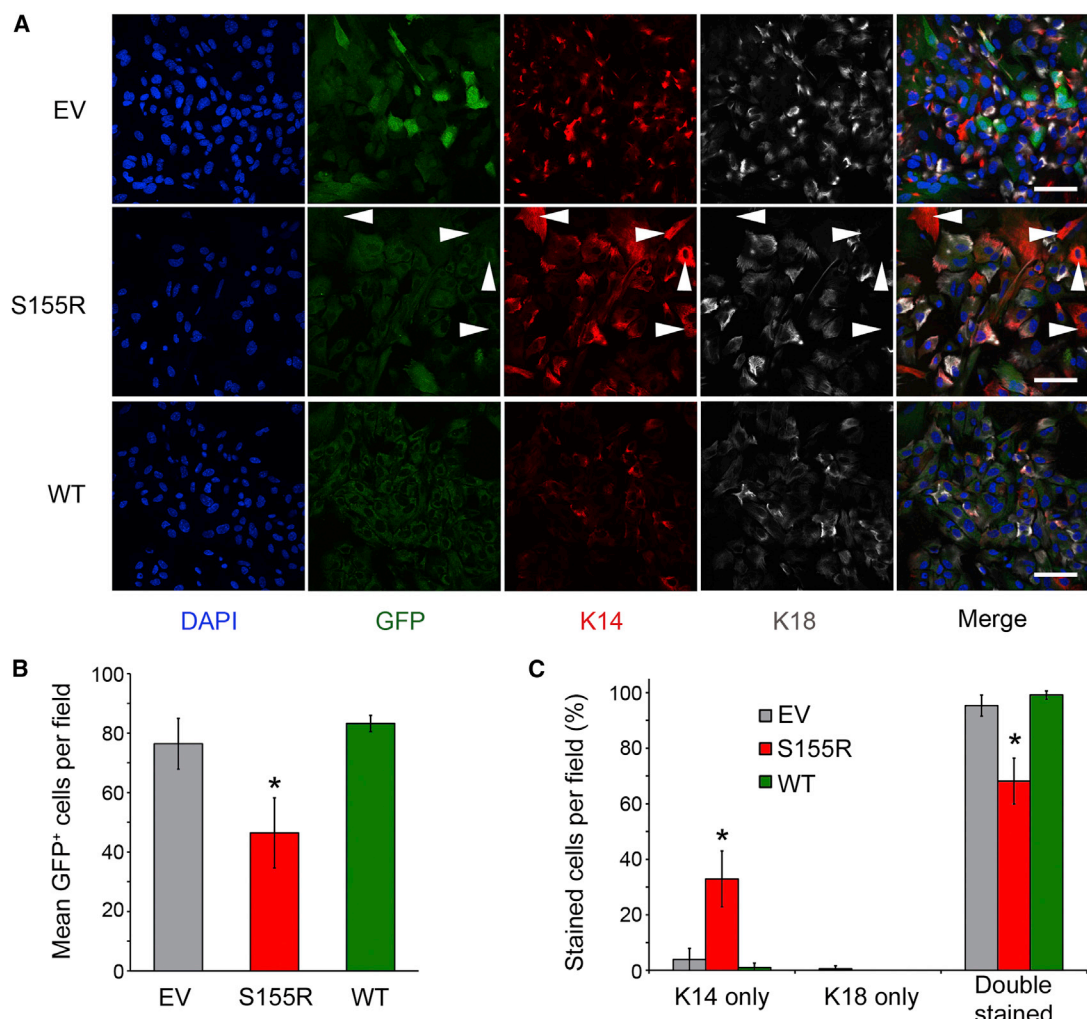


Figure 2. AURKA Regulates Proliferation and Differentiation of Mammary Epithelial Cells In Vitro

(A) Immunofluorescence staining of primary mouse mammary epithelial cells transduced with control EV (top row), S155R (middle row), or WT (bottom row) lentivirus that also express GFP. Cells were stained for the basal marker K14 (red) and the luminal marker K18 (gray) and counterstained with DAPI (blue) (scale bars, 30 μ m). Arrowheads indicate K14⁺-only cells. See Figure S3 for localization of AURKA to mitotic spindles of transduced cells and Figure S4 for examples of staining with the additional basal/myoepithelial markers K5 and α SMA.

(B) Mean (\pm SD) number of transduced GFP⁺ mammary epithelial cells per field of view. Data are from three independent cell preparations after 10 days in culture (each of which had ten fields of view from three separate coverslips counted). Identical numbers of cells were plated per well in all cultures. *p < 0.05 (t test) showing a significantly lower cell number in S155R cultures versus control (EV) and WT cells.

(C) Mean (\pm SD) number of GFP⁺ and K14⁺, GFP⁺ and K18⁺, or GFP⁺ and K14⁺/K18⁺ mammary epithelial cells per field of view. Data are from three independent cell preparations after 10 days in culture (each of which had ten fields of view over three separate coverslips counted). Identical numbers of cells were plated per well in all cultures. *p < 0.05 (t test on Log₁₀-transformed data).

See also Figures S3 and S4.

AURKA expression affected this promiscuous expression of lineage markers, the number of cells expressing K14 only, K18 only, or coexpressing both K14 and K18 in the lentivirus-transduced cultures was determined (Figure 2C). A total of 95.32% \pm 3.79% (mean \pm SD) of EV- and 99.15% \pm 1.47% of WT-transduced cells stained for both K14 and K18. However, only 68.18% \pm 8.23% of S155R-transduced cells were double positive for K14 and K18 (p < 0.05 t test on Log₁₀-transformed data versus EV and WT-transduced cells). The remaining S155R-transduced cells were K14⁺ only (32.9% \pm 10.07%) and

had a more flattened, spread appearance than K14⁺/K18⁺ cells (Figure 2A, arrowheads). Furthermore, staining of the cultures with two markers of mammary myoepithelial cells, keratin 5 (K5) and α -isoform smooth muscle actin (SMA), demonstrated that whereas S155R-transduced cells could express both K5 and SMA, EV and WT-expressing cells were K5 and SMA negative (Figure S4). Therefore, these data not only demonstrated that S155R AURKA reduced proliferation of mammary epithelial progenitors in vitro but also suggested that it promoted differentiation along the basal myoepithelial lineage.

In Vivo Expression of S155R in the Mouse Mammary Epithelium Causes Cells to Accumulate in the Myoepithelial Lineage

To examine the role of AURKA in mammary epithelial cell fate determination *in vivo*, freshly harvested primary mouse mammary epithelial cells were transduced with the EV, S155R, or WT lentiviruses and transplanted at equal numbers into cleared mammary fat pads of syngeneic mice. Eight weeks after transplantation, the fat pads were removed and examined (Figures 3A and 3B). GFP-labeled mammary epithelial outgrowths were observed in 10 out of 30 fat pads transplanted with EV or WT-expressing cells and in 9 out of 30 fat pads transplanted with S155R-expressing cells. However, whereas EV and WT outgrowths were extensive and filled $\geq 50\%$ of the fat pad in six and seven outgrowths, respectively, S155R outgrowths were rudimentary (Figure 3A). Analysis of sections of EV, WT, and S155R outgrowths stained for myoepithelial (K5 and SMA) and luminal (K18 and K19) markers also revealed morphological differences (Figures 3C–3E, S5A, and S5B). EV and WT outgrowths displayed a typical normal mammary epithelial morphology with distinct myoepithelial (K5 and SMA positive) and luminal (K18 and K19 positive) layers. In contrast, the S155R outgrowths typically consisted of only a single layer of myoepithelial cells that expressed little or no luminal keratin.

The limited extent of the outgrowths produced by the S155R-transduced cells suggested that whereas these cells were as transplantable as the control cells, their ability to proliferate and/or properly differentiate was impaired. To further characterize differentiation defects in the outgrowths, cells isolated from transplanted fat pads were analyzed by flow cytometry to determine the proportions of the different mammary epithelial cell types (Figures 3F–3I). GFP⁺ cells isolated from control fat pads (Figure 3G) had a flow cytometric profile similar to GFP⁺ cells from the same preparations or to transplanted nontransduced epithelial cells (Figure 3F). However, GFP⁺ cells isolated from S155R fat pads (Figure 3H) were significantly shifted into the CD24^{+/Low} Sca-1⁻ basal myoepithelial population (which formed $9.3\% \pm 1\%$ of the GFP⁺ control cells but $40.4\% \pm 5.4\%$ of the GFP⁺ S155R cells; mean \pm SD, n = three independent transplant experiments; p < 0.0001 t test on Log₁₀-transformed data) (Figure 3J).

There was no significant difference between the size of the basal myoepithelial GFP⁺ populations isolated from WT (Figure 3I) and control fat pads. However, the size of the differentiated luminal CD24^{+/High} Sca-1⁺ population was significantly decreased in the WT outgrowths compared to EV controls ($42.13\% \pm 1.35\%$ of GFP⁺ EV cells and $20.33\% \pm 0.58\%$ of GFP⁺ WT cells; mean \pm SD, n = three independent transplant experiments; p < 0.0001 t test on Log₁₀-transformed data), and the size of the luminal CD24^{+/High} Sca-1⁺ progenitor-enriched population was significantly increased ($32.36\% \pm 4.07\%$ of GFP⁺ EV cells and $43\% \pm 4.8\%$ of GFP⁺ WT cells; mean \pm SD, n = three independent transplant experiments; p < 0.05 t test on Log₁₀-transformed data) (Figure 3J).

Next, to determine whether AURKA not only regulated the fate of differentiating mammary cells but also self-renewal of mammary stem cells, serial transplants were carried out. Primary

mammary epithelial cells were isolated from mice carrying a red fluorescent protein (RFP) transgene driven by the K14 promoter (*K14-RFP*). These were transduced with the EV, S155R, or WT lentiviruses and transplanted into cleared mammary fat pads. After 8 weeks, the fat pads were harvested, successful RFP⁺ transplants were scored, and the extent of the GFP expression within each RFP⁺ outgrowth was determined (Figure S5C). Frozen sections taken from small biopsies of the outgrowths were used to confirm coexpression (Figures S5D and S5E). Having scored RFP and GFP staining in the unfixed tissue, the transplanted fat pads were digested to single cells, and the cells were retransplanted into cleared fat pads at equal numbers. Note that cells were not sorted to purify out the GFP⁺ cells from the first round of transplantation because this can have deleterious effects on transplant potential.

In the first round of transplants, as previously, no differences in the number of EV, S155R, or WT outgrowths were observed, suggesting that there was no effect on initial engraftment. Again, however, the S155R outgrowths were less extensive. In the second round of transplants, whereas both the EV and WT-expressing cells engrafted successfully and with equal potency, only a single rudimentary S155R outgrowth formed (Figure 3K), suggesting that the self-renewal of mammary stem cells expressing S155R in the primary graft had been inhibited. Overall, therefore, these data supported a model in which WT AURKA activity enriched for cells with a luminal progenitor phenotype, whereas expression of mutant S155R AURKA promoted the basal myoepithelial cell fate while suppressing stem cell self-renewal.

AURKA Regulates Mitotic Spindle Orientation in the Mammary Epithelium

Next, we addressed potential mechanisms by which AURKA may regulate mammary epithelial cell fate and differentiation. In *Drosophila* neuroblasts, AURKA regulates asymmetrical divisions and cell fate by promoting alignment of the mitotic spindle with the cortical polarity axis (Lee et al., 2006). We therefore investigated a role for AURKA in regulating the orientation of the mitotic spindle in the cap cells of TEBs.

We examined mitotic spindle orientations in cap cells of the unmanipulated developing pubertal mammary gland (Figure 4A) and in the invading ductal ends of outgrowths developing from transplanted mammary epithelial cells transduced with EV, WT (Figures 4B and 4C), or S155R lentiviruses. Spindle orientations were classed as parallel or perpendicular to the border of the basal cell layer with the stroma. The total number of mitotic figures in each TEB was also determined. In unmanipulated glands, 36.6% of mitoses observed in TEBs were at the epithelium-stroma border (393 mitoses observed in total, 144 at the border). Mitoses aligned parallel to the border formed $21.97\% \pm 1.71\%$ of the total number observed, whereas mitoses aligned perpendicular to the border formed $14.8\% \pm 1.06\%$ of the total number. Fewer mitoses were observed in control EV-transplanted glands (97 mitoses, of which 31 were at the border), but the proportion of parallel ($16.71\% \pm 6.54\%$ of the total number) and perpendicular ($16.65\% \pm 1.78\%$ of the total number) divisions at the epithelium-stroma border was not significantly different from the unmanipulated gland. However, in WT glands, there was an

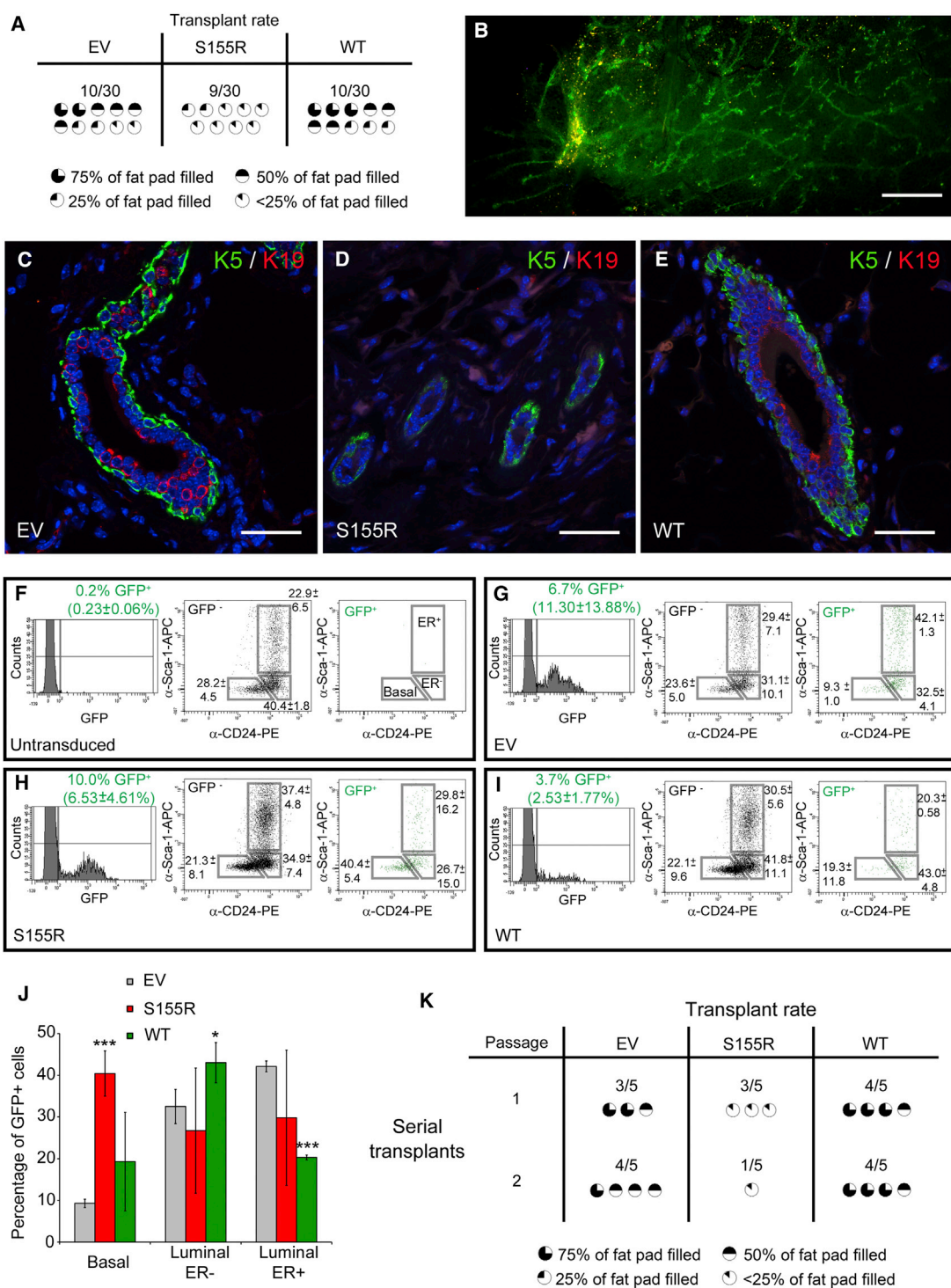


Figure 3. AURKA Regulates Mammary Epithelial Differentiation In Vivo

(A) Transplant of mammary epithelial cells transduced with EV, S155R, or WT viruses from three independent transplant sessions. The number of successful GFP⁺ outgrowths as a fraction of the number of transplanted fat pads is given. The extent to which each outgrowth filled the fat pad is indicated by the “pie chart” symbols.

(B) Whole mount of fat pad transplanted with WT-transduced cells. Scale bar, 3 mm.

(C–E) Sections through cleared fat pad outgrowths transduced with EV (C), S155R (D), or WT (E) viruses. Sections were double stained for K5 and K19 expression and counterstained with DAPI. Note the predominantly single layer of K5-positive/K19-negative epithelium in the S155R outgrowth. Scale bars, 40 μm. See Figure S5 for additional sections stained for K18 and SMA expression.

(legend continued on next page)

increase in the proportion of divisions occurring perpendicular to the epithelium-stroma border ($26.65\% \pm 1.57\%$ of the total number) and a decrease in parallel divisions ($6.22\% \pm 3.34\%$; 125 mitoses, of which 41 were at the border; **Figure 4C; Table 1**).

Unfortunately, no mitoses could be observed in sections from the small S155R outgrowths. Therefore, to determine how S155R AURKA might influence the direction of cell divisions, we used an *in vitro* three-dimensional (3D) culture model that mimics the *in vivo* morphology of the mammary epithelium (Bissell et al., 2003). Freshly isolated EV-, S155R-, and WT-transduced mammary epithelial cells were plated at low density, at equal numbers, on growth factor-reduced Matrigel and cultured for 4 days to allow growth of 3D colonies (**Figure 4D**). Cultures were then fixed, stained for tubulin and with DAPI, and the orientation of cell divisions was determined. In colonies derived from control cells, $42.46\% \pm 2.85\%$ of divisions were parallel, and $57.53\% \pm 5.47\%$ were perpendicular to the basement membrane (mean \pm SD, n = 73). Strikingly, however, S155R promoted more parallel and fewer perpendicular divisions ($68.11\% \pm 2.21\%$ and $31.88\% \pm 3.01\%$, respectively; mean \pm SD, n = 69), whereas WT AURKA had the opposite effect, increasing perpendicular divisions and decreasing parallel divisions ($84.21\% \pm 4.22\%$ and $15.78\% \pm 2.27\%$, respectively; mean \pm SD, n = 76) (**Figure 4E**).

To determine whether expression of S155R altered proliferation in these cultures as in monolayer cultures and *in vivo* outgrowths, 10-day-old Matrigel cultures of EV-, S155R-, and WT-transduced cells were assayed for differences in final cell numbers. As expected, there were significantly fewer cells in cultures obtained from S155R-expressing cells than EV or WT cultures (**Figure 4F**). This was not a result of an increase in apoptosis in these cultures because there was no observable increase in the number of pyknotic nuclei in the S155R colonies (**Table S1**).

To analyze whether AURKA-dependent alterations in mitotic spindle orientation correlated with altered mammary epithelial differentiation *in vitro* as it did *in vivo*, we examined the expression of genes associated with the myoepithelial (*Acta2*, *Fzd1*, *Fzd2*, *Itga6*, *Kitl*, *Krt14*, *Snai2*, *Tsp63*, *ΔNp63*, and *Vim*) and luminal (*Cd14*, *Erbb3*, *Esr1*, *Kit*, *Krt18*, *Lyn*, *Pgr*, and *Prlr*) lineages, together with three genes that are not differentially expressed in the mammary epithelium (*Brca1*, *Gata3*, and *Itgb1*) (Kendrick et al., 2008; Regan et al., 2012) (**Figure S6**). Overall, S155R transduction resulted in a reduction in transcriptional activity relative to control-transduced cells, consistent with terminal differentiation, whereas WT AURKA transduction resulted in an overall increase in transcriptional activity. Notably, how-

ever, expression of *ΔNp63*, a key regulator of the basal epithelial lineage (Romano et al., 2009; Carroll et al., 2006), was upregulated in S155R-expressing cells. Furthermore, the two most highly upregulated genes in WT-transduced cultures were *Prlr* and *Cd14*, both of which are markers of luminal progenitors (Kendrick et al., 2008).

These data demonstrate that AURKA regulates mitotic spindle orientation in the mammary epithelium. High AURKA activity promotes divisions perpendicular to the basement membrane and, consistent with this, leads to an increase in the proportion of luminal progenitor cells. The S155R mutant, in contrast, promotes divisions parallel to the basement membrane, resulting in an increase in differentiated basal myoepithelial cells.

AURKA Regulates NOTCH Signaling in Mammary Epithelial Cells

In *Drosophila* sensory organ precursor cells, AURKA regulates daughter cell fate both through mitotic spindle alignment and asymmetric intracellular localization of NUMB, a negative regulator of NOTCH signaling (Lee et al., 2006). NOTCH signaling is also a key regulator of mammary stem/progenitor cells and promotes luminal differentiation in the mammary epithelium (Bouras et al., 2008; Buono et al., 2006; Harrison et al., 2010). We therefore examined whether there was a relationship between AURKA, mitotic spindle orientation and NOTCH signaling in the mammary epithelium.

We initially examined NUMB localization. However, in 4-day-old 3D cultures of EV-, S155R-, and WT-transduced primary mammary epithelial cells, no correlation was observed between endogenous NUMB localization or expression and either S155R or WT AURKA (**Figure S7**).

To determine whether AURKA may regulate NOTCH signaling independently of NUMB, expression levels of the ligands (*Dll1*, *Jag1*, and *Jag2*) and the receptors (*Notch1*–*Notch4*) were examined in EV-, S155R-, and WT-transduced mammary epithelial cells in 3D culture (**Figure 5**). Signaling through the pathway was monitored through target gene (*Hes1*, *Hes6*, *Hey1*, *Hey2*, and *Twist1*) expression. S155R expression resulted in decreased *Dll1*, *Jag1*, *Jag2*, *Notch1*, *Notch3*, and *Notch4* levels, whereas WT expression increased expression of *Notch1*, *Notch2*, and *Notch3*. These differences were reflected in profound changes in expression of NOTCH target genes. S155R expression resulted in a strong suppression of *Hes1*, *Hes6*, and *Twist1* expression, whereas WT expression resulted in a strong increase in expression of all five target genes tested. Consistent with the NUMB protein expression data, there were no differences in *Numb* gene expression between EV-, S155R- and WT-

(F–I) Flow cytometric analysis of cells prepared from fat pads transplanted with virus-transduced cells. Cells were gated on GFP expression and then CD24 and Sca-1 staining to determine the population distributions of GFP[−] and GFP⁺ cells (indicated by the “Basal,” “ER[−],” and “ER⁺” regions in F). The percentages of GFP⁺ cells in the representative experiment shown are indicated, together with the mean (\pm SD) percentages of GFP⁺ epithelial cells from all three experiments. Note that the relatively low percentages of GFP⁺ cells may be a result of an immune response to GFP by the syngeneic transplant hosts (J.L.R., K.S., and M.J.S., unpublished data). (F) Untransduced cells. (G) GFP⁺ EV-transduced cells. (H) S155R-transduced cells. (I) WT-transduced cells.

(J) Data from (G)–(I) on the distribution of GFP⁺ cells in the three main epithelial populations expressed as a bar chart (mean \pm SD) for direct comparison. Asterisks indicate significant changes (t test on Log₁₀-transformed data) in size of each population relative to EV transplant (gray bars). *p < 0.05; **p < 0.001.

(K) Rates of transplantation and extent of GFP⁺/mRFP⁺ outgrowths across two rounds of serial transplantation of virus-transduced mRFP⁺ cells. See **Figure S5** for images of outgrowths.

See also **Figure S5**.

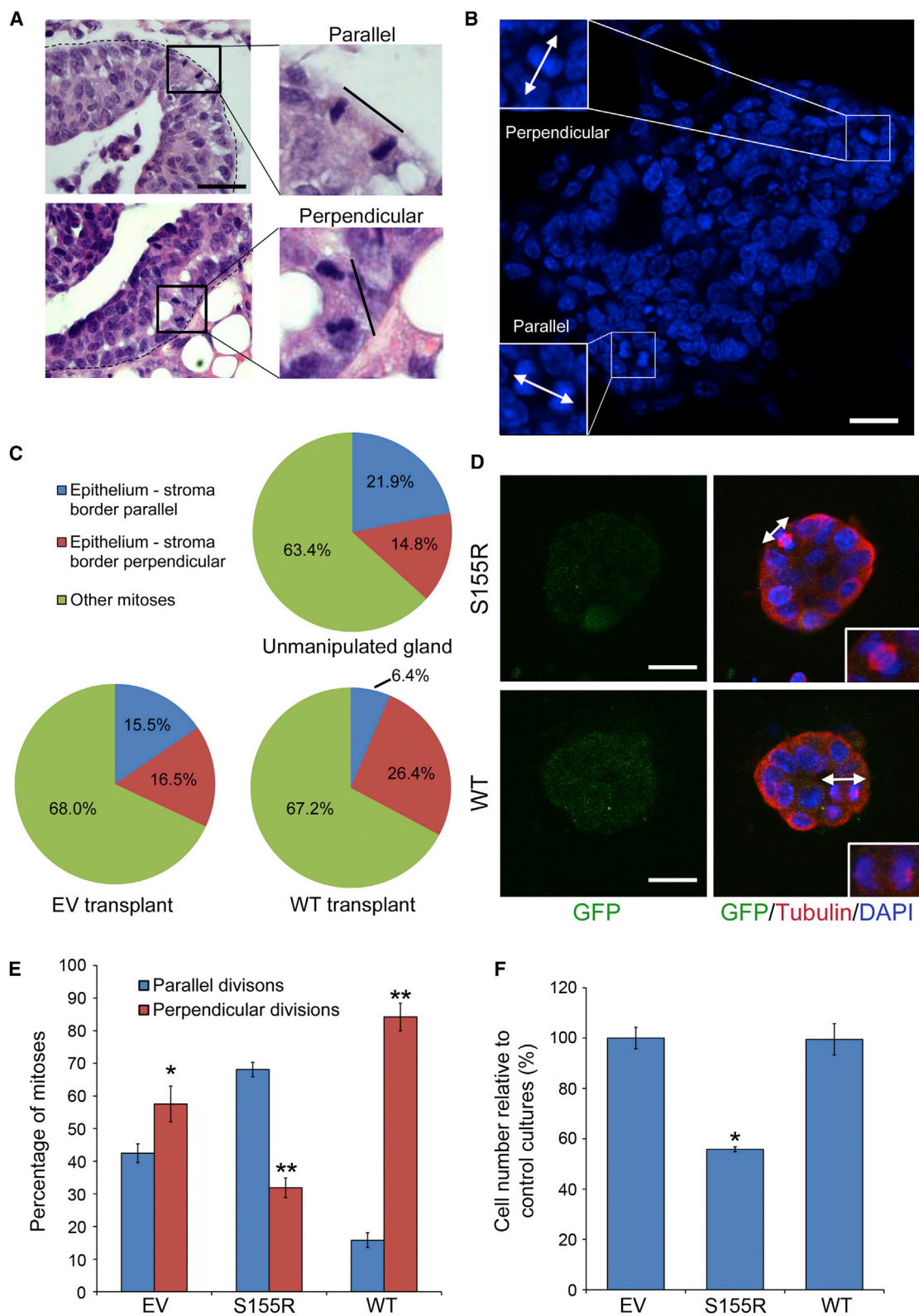


Figure 4. AURKA Regulates Mitotic Spindle Orientation

(A) H&E TEBs showing divisions parallel and perpendicular to the border with the mammary stroma. Scale bar, 35 μ m.

(B) DAPI-stained section of TEB from WT-transplanted fat pad showing examples of parallel and perpendicular mitoses. Scale bar, 8 μ m.

(legend continued on next page)

Table 1. Mitotic Spindle Counts

Mouse	N	Stroma Border		Others	Total
		Para	Perp		
1	4	28	19	93	140
2	6	34	23	92	149
3	4	24	16	64	104
				393	
Virus	Tx				
EV	1	3	5	4	13
	2	3	4	7	30
	3	3	6	5	23
S155R AURKA	1	3	0	0	0
	2	3	0	0	0
	3	3	0	0	0
WT AURKA	1	3	1	9	22
	2	3	3	13	36
	3	3	4	11	26
				222	

Number, localization, and orientation of mitoses counted in biopsies of unmanipulated tissue (upper) and virus-transduced transplanted material (lower). “N” indicates number of fat pads examined in each of three unmanipulated mice (upper) or in material derived from each of three independent transplant sessions (Tx) (lower). Para, parallel divisions. Perp, perpendicular divisions.

transduced cultures (Figure 5). In contrast, Hedgehog signaling (a second pathway important for mammary development and cancer) (Kasper et al., 2009; Visbal and Lewis, 2010) showed no change in activity in response to either S155R or WT expression (Figure S8).

AURKA Regulation of Mitotic Spindle Orientation Is NOTCH Dependent

Our results placed both mitotic spindle orientation and NOTCH signaling downstream of AURKA. However, they did not establish a direct link between spindle orientation and NOTCH signaling. To determine whether such a link existed, we first established whether NOTCH signaling was active in the developing TEBs by staining sections for the active cleaved fragment of the NOTCH1 receptor, the Notch intracellular domain 1 (NICD1). NOTCH1 activity in particular is correlated with poor prognosis breast cancer (Parr et al., 2004; Reedijk et al., 2005). Serial sections through TEBs were stained for NICD1 and the basal marker

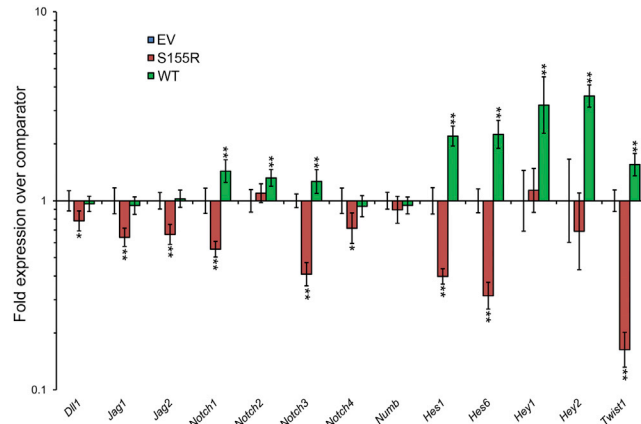


Figure 5. AURKA Regulates NOTCH Signaling

Relative expression by quantitative real-time reverse-transcription PCR of NOTCH ligands (*Dll1*, *Jag1*, and *Jag2*), receptors (*Notch1–Notch4*), *Numb*, and target genes (*Hes1*, *Hes6*, *Hey1*, *Hey2*, and *Twist1*) in EV, S155R, and WT-transduced 3D cultures. Data are presented as mean fold expression (± 95 confidence limits) relative to comparator sample (EV-transduced cells). Data are from three independent experiments. Significant differences are * $p < 0.05$ and ** $p < 0.01$ and were determined by inspection of error bars as described by Cumming et al. (2007). See Figure S7 for analysis of NUMB localization and expression levels and Figure S8 for analysis of expression of Hedgehog signaling pathway components in response to AURKA expression.

K5. General cytoplasmic NICD1 staining was observed in the TEBs, together with brightly punctate nuclear staining in a subset of cells. Both luminal and basal cells were stained (Figures 6A and S9A).

To directly test whether inhibition of NOTCH pathway activity would affect mitotic spindle orientation in the TEBs, 3-week-old mice were treated with the γ secretase inhibitor (GSI) RO4929097, or with vehicle only, daily for 5 days. Mammary fat pads were then harvested and either fixed for histological analysis, or mammary epithelial cells were processed for extraction of RNA. To confirm that GSI treatment had suppressed NOTCH signaling, sections through TEBs were stained for NICD1 expression, and *Hes1* gene expression was analyzed by quantitative real-time reverse-transcription PCR. As expected, GSI-treated animals had weaker NICD1 staining and lower levels of *Hes1* gene expression than control animals, confirming suppression of NOTCH signaling (Figures 6B, S9B, and S9C). Next, mitotic spindle orientations were counted as previously in the vehicle- and control-treated TEBs. Remarkably,

(C) Orientation of mitoses (parallel, perpendicular, or “Other”) in TEBs as a percentage of the total number of mitoses counted in 14 unmanipulated mammary fat pads ($n = 7$ mice), 9 fat pads transplanted with cells transduced with EV virus ($n = 3$ separate transplant sessions), and 9 fat pads transplanted with WT virus ($n = 3$ transplant sessions). See Table 1 for details.

(D and E) Primary mammary epithelial cells were transduced with EV, S155R, or WT viruses and cultured as 3D colonies. (D) Colonies were fixed after 4 days and stained with anti- α -tubulin (red) and DAPI (blue) and orientations of mitoses determined. Scale bars, 20 μ m. (E) Mitotic orientations relative to the extracellular matrix for 3D virus-transduced colonies. Data are expressed as the percentage (mean \pm SD; data are from three independent experiments, each of which examined eight separate wells for each virus) of parallel and perpendicular divisions observed in each set of virus-transduced cultures. * $p < 0.05$, ** $p < 0.01$ (t test on Log₁₀-transformed data).

(F) Cell number in 3D cultures after transduction with EV, S155R, or WT viruses. Data are expressed as percentage (mean \pm SD; data are from three independent experiments) of viable cells relative to EV-transduced 3D cultures. * $p < 0.05$ (t test on Log₁₀-transformed data). See Figure S6 for analysis of expression of lineage-associated genes in 3D cultures following virus transduction.

See also Figure S6.

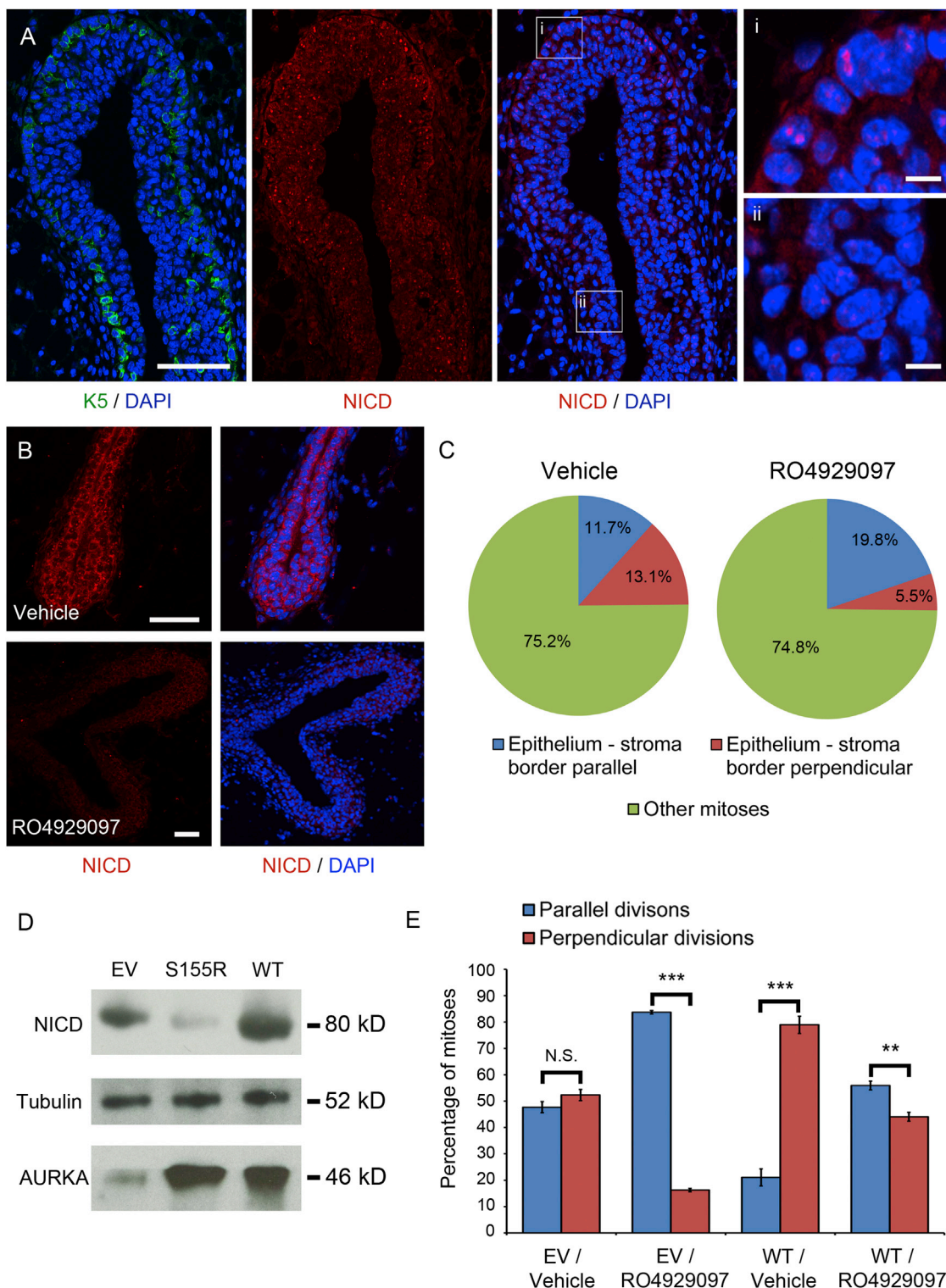


Figure 6. AURKA Regulation of Mitotic Spindle Orientation Is Dependent on NOTCH Signaling

(A) Localization of the NICD1 in the TEBs of 4-week-old mouse mammary epithelium. Punctate NICD1 staining was observed in a subset of cells in the TEBs, including the basal cell layer (magnified regions i and ii). Scale bar, 50 μ m. Scale bars in magnified regions, 4 μ m.

(B) NICD1 staining of TEBs from 4-week-old mice treated with vehicle only (top) or the GSI RO4929097 (bottom). Scale bars, 60 μ m. See Figure S9 for additional images and for quantitative real-time reverse-transcription PCR analysis of *Hes1* gene expression in tissue taken from vehicle- and GSI-treated mice and 3D cultures.

(legend continued on next page)

GSI-treated TEBs showed a shift from perpendicular to parallel divisions in the outer layer of cells of the TEBs, bordering the stroma, mimicking the effects of S155R (**Figures 6C and S9D**).

Next, we examined the relationship between AURKA and NOTCH in the 3D in vitro culture system. Western blot analysis of NICD1 and AURKA levels in cultures transduced with EV, S155R, or WT viruses demonstrated that S155R suppressed NICD1 levels and therefore NOTCH signaling (**Figure 6D**), consistent with the quantitative real-time reverse-transcription PCR data (**Figure 5**). Finally, we determined whether NOTCH signaling was required for the effects of AURKA on spindle orientation. 3D cultures transduced with either EV or WT virus were treated with vehicle or GSI. As previously, WT transduction resulted in a shift from similar numbers of perpendicular and parallel divisions in control cultures to a significant increase in the proportion of perpendicular divisions. In contrast, as was observed in vivo, GSI treatment of control cells resulted in a significant increase in the proportion of parallel divisions, mimicking the effects of S155R. Furthermore, GSI treatment of WT-transduced cells blocked the increase in perpendicular divisions seen with WT alone (**Figure 6E**). These findings provide strong evidence that AURKA regulates mitotic spindle orientation in the mammary epithelium, in particular in TEBs in the developing gland, and that this regulation is mediated directly through NOTCH signaling.

DISCUSSION

We have demonstrated a role for AURKA in regulating cell fate in the mammary epithelium. AURKA regulated mitotic spindle orientation in the TEBs and thus governed the position of daughter cells and their interactions with the microenvironment. The regulation of mitotic spindle orientation was NOTCH signaling dependent because, first, in a 3D model culture system, WT AURKA overexpression activated the NOTCH signaling pathway, whereas expression of S155R AURKA suppressed NICD1 levels. Second, use of the GSI RO4929097 in vitro and, notably, in vivo mimicked the effects of S155R AURKA expression, promoting cell divisions that were parallel to the basement membrane and blocking perpendicular divisions. Third, combining the GSI with WT AURKA overexpression rescued the effects of WT AURKA alone and restored the balance between perpendicular and parallel divisions. We therefore suggest a model in which AURKA activity in the cap cells of the TEBs promotes divisions perpendicular to the border with the mammary stroma and that this is mediated through active NOTCH signaling. Such perpendicular divisions will result in one daughter cell that enters the body cell/luminal lineage and one daughter cell that stays basal. In contrast, if AURKA activity does not activate NOTCH signaling, then the divisions will be

parallel to the border: both daughter cells will stay in the basal layer and enter the myoepithelial lineage. Exactly how AURKA couples to the NOTCH pathway remains to be determined, however. Although there are caveats associated with overexpression of mutant proteins such as the S155R, the facts that it is a mutant associated with human cancer (The Cancer Genome Project, <http://www.sanger.ac.uk/genetics/CGP/cosmic/>) and that use of a small molecule NOTCH inhibitor phenocopied the effects of S155R overexpression both in vitro and in vivo strongly support the physiological relevance of our findings.

Spindle alignment depends on myosin motors in the cortex and astral microtubules (MTs), which link the centrosomes to the cell cortex during mitosis (Siller and Doe, 2009). Astral MT function is regulated by the PAR polarity complex (McCaffrey and Macara, 2011) and also depends on AURKA because the astral MTs are short and sparse when AURKA is disabled (Giet et al., 2002). It is likely that AURKA - astral MT - myosin motor mechanisms position centrosomes not only with respect to each other but also in response to external cues. The nature of these external cues is unknown, but it is intriguing that targeted deletion of the β 1-integrin to the basal compartment of the mouse mammary gland resulted in a change in spindle orientations in the basal cell layer of the intact gland during pregnancy-driven proliferation from parallel to the basement membrane to random orientations. Furthermore, there was a decrease in stem cell self-renewal as demonstrated by loss of potency in serial transplantation (Taddei et al., 2008). Taken together, these findings support a model in which mitotic spindle orientation, regulated by AURKA, NOTCH, and β 1-integrin, is a key mechanism of mammary stem cell self-renewal and cell fate determination. Further studies will be needed to determine how AURKA activates NOTCH signaling and how NOTCH signaling regulates centrosomal positioning and thus spindle orientation. It is also unclear at this time whether the AURKA - NOTCH - mitotic spindle orientation pathway is specific only for basal cells or is potentially active in both basal and luminal cells.

Recent lineage analysis of the mouse mammary gland has suggested that from 4 weeks postpartum onward (approximately 1 week into puberty), the basal and luminal epithelial lineages are separate and maintained by their own stem and/or progenitor compartments (Van Keymeulen et al., 2011). However, it is unclear to what extent the labeling strategies used in these studies labeled cap cells of the TEBs. Although our in vivo studies were carried out on slightly younger animals (3–4 weeks old), they demonstrated that cap cells in the TEBs can contribute to either the basal cells of the subtending duct or to the body cells (and thus to the luminal layer). Whether or not the daughter cells contributed to the luminal or basal lineages was determined by spindle orientation. Notably, our findings provide mechanistic insights into previous observations that cap cells can contribute

(C) Location and orientation of mitoses in TEBs as a percentage of the total number of mitoses counted in ten mammary fat pads from five vehicle-treated mice and ten fat pads from five GSI-treated mice. See **Figure S9** for details.

(D) Western analysis of NICD1 and AURKA expression in 3D cultures transduced with EV, S155R, or WT virus.

(E) Mitotic orientations relative to the extracellular matrix for 3D colonies transduced with EV or WT virus and cultured with either vehicle or GSI. Data are expressed as the percentage (mean \pm SD; data are from three independent experiments, each of which examined 16 separate wells for each condition) of parallel and perpendicular divisions observed under each condition. ** p < 0.01, *** p < 0.001 (t test on Log₁₀-transformed data). See also **Figure S9**.

to both cell lineages (Srinivasan et al., 2003; Williams and Daniel, 1983).

Our findings support the model that the TEBs do contain a common stem cell for both the luminal and basal cell layers and that the balance between the lineages is regulated by the orientation of the divisions of the cap cells, under the control of AURKA and NOTCH signaling. Once the ducts have properly formed, maintaining the basal and luminal epithelial cells as separate lineages requires cell divisions in the basal layer to be parallel to the basement membrane, which will occur if NOTCH signaling is blocked. However, during alveologenesis, basal cells may contribute to the luminal layer (van Amerongen et al., 2012). Our findings show that this could be achieved by activating NOTCH signaling in dividing basal cells, causing orientation to switch from parallel to perpendicular.

NOTCH signaling is an important pathway in mammary epithelial development and regulates mammary epithelial cell fate (Bouras et al., 2008; Buono et al., 2006). Expression of *Notch1*-*Notch3* is associated with luminal cells (Bouras et al., 2008; Kendrick et al., 2008), but *Notch4* expression has been associated with stem cells and the regulation of self-renewal properties in cancer cells (Harrison et al., 2010). In human breast cancer, NOTCH1 expression correlates with poor prognosis and “basal-like” breast cancers but NOTCH2 with good prognosis and the luminal ER+ phenotype (Parr et al., 2004; Reedijk et al., 2005; Lee et al., 2008).

A number of primary human tumors have been identified carrying AURKA mutations (S155R in colon, H86Y in breast, L318V in ovary, and S398L and S361* nonsense in lung) (Bibby et al., 2009) (The Cancer Genome Project, <http://www.sanger.ac.uk/genetics/CGP/cosmic/>), and AURKA is expressed at high levels in a range of tumors (Bischoff et al., 1998; Torchia et al., 2009; Zhou et al., 1998). In primary breast cancer samples, high AURKA expression is usually associated with the basal-like subtype (Yamamoto et al., 2009). This subtype tends to develop in carriers of mutations in the BRCA1 tumor suppressor gene (Da Silva and Lakhani, 2010). Intriguingly, mutations in the BRCA1 RING domain are associated with centrosomal amplification in breast cancer (Kais et al., 2012), and AURKA activity is required not only for centrosome amplification (Leontovich et al., 2013; Zhou et al., 1998) but also for ILK-dependent centrosomal clustering and the formation of pseudobipolar mitotic spindles in cells with amplified chromosomes (Fielding et al., 2011). If NOTCH pathway activity is required for AURKA-dependent centrosome clustering in tumors, then the use of GSIs in BRCA1 tumors has potential as a therapy to inhibit clustering and drive mitotic catastrophe as a result of multipolar divisions. Our findings also suggest that AURKA/NOTCH-dependent regulation of spindle orientation could contribute to the recently proposed cell translocation mechanism that allows tumor cells to evade microenvironments that suppress neoplastic activity (Leung and Brugge, 2012).

Finally, both AURKA and NOTCH signaling have attracted much interest in recent years as potential therapeutic targets in cancer. Our results suggest that combination therapies of AURKA inhibitors and GSIs may offer synergistic results. Whether these results will be synergistic benefits or toxicities, however, remains to be determined.

EXPERIMENTAL PROCEDURES

Preparation of Mammary Epithelial Cells for Flow Cytometry

All animal work was carried out under UK Home Office project and personal licenses following local ethical approval and in accordance with local and national guidelines. Single cells were prepared from fourth mammary fat pads of 10-week-old virgin female FVB mice (Regan et al., 2012) and stained with anti-CD24-FITC, anti-Sca-1-APC, anti-CD45-PE-Cy7, anti-CD49f-PE-Cy5, and anti-c-Kit-PE. Mammary epithelial cell subpopulations were defined as shown in Figures 1 and S1.

Gene Expression Analysis by Quantitative Real-Time Reverse-Transcription PCR

Freshly sorted primary cells were lysed in RLT buffer (QIAGEN) and stored at -80°C. Total RNA was extracted using an RNeasy MinElute Kit (QIAGEN), according to the manufacturers' instructions. For cultured cells, RNA was isolated with TRIzol (Invitrogen). Quantitative real-time reverse-transcription PCRs were performed as previously described (Kendrick et al., 2008). For comparison of *Aurka*, *Ccnd1*, and *Ccnb1*, a SYBR Green-based method with custom-designed primers (Primer3v.0.4.0; <http://frodo.wi.mit.edu/primer3>) was used. All results were calculated using the Δ-ΔCT method. Data were expressed as the mean fold gene expression difference in three independently isolated cell preparations over a comparator sample with 95% confidence intervals.

Lentivirus Production and Transduction of Primary Cells

Lentiviruses were produced using the Tronolab (<http://tronolab.epfl.ch/>) pWPI system. For two-dimensional culture and transplantation assays, primary mammary cells were transduced with virus using the suspension method as described (Kendrick et al., 2008). For 3D Matrigel culture, primary mammary cells were suspended in viral supernatants and seeded in wells containing prepared Matrigel gels (as above). After 16 hr, wells were washed and refed and then transferred to low-oxygen culture conditions.

Mammary Epithelial Cell Transplantation

Transplantation of lentivirus-transduced primary mouse mammary epithelial cells isolated from FVB and K14-mRFP mice (a kind gift of Elaine Fuchs, Rockefeller University) (Zhang et al., 2011) into cleared fat pads of 3-week-old syngeneic FVB and athymic Nude mice, respectively, was carried out as described by Sleeman et al. (2007). For analysis of GFP/RFP serial transplants, 10 mm frozen sections were fixed, incubated with DAPI, and then postfixed before being mounted. Sections were viewed on a Leica TCS SP2 confocal microscope.

Histological Analysis

The 3-week-old intact WT FVB mouse mammary fat pads were whole mounted and fixed. They were then cut transversely into four strips that were paraffin embedded by standard methods. H&E sections of each strip were used to locate the TEBs for mitotic figure counting. Parallel divisions were defined as those at the reference surface that would leave both daughter cells in the same position relative to that surface. Perpendicular divisions were defined as those at the reference surface that left one daughter cell closer to and one further from that surface. Mitotic figures that could not be related to a reference surface (“other mitoses”) were simply counted.

Use of GSIs

For in vivo use, the GSI RO4929097 was formulated as a suspension in 1.0% (hydroxypropyl)methyl cellulose (HPMC) (Sigma-Aldrich) in water with 0.2% Tween 80 for oral administration. RO4929097 was dosed once daily at 10 mg/kg for 5 days. After 5 days, fourth mammary fat pads from vehicle-treated and RO4929097-treated groups were whole mounted and fixed in 4% formalin overnight, processed, paraffin embedded, and serial sectioned prior to immunostaining for NICD1 (Abcam; ab8925) and DAPI. Mitotic spindle orientations were counted as above.

Third mammary fat pads from vehicle-treated and RO4929097-treated groups were processed to single cells and stained for CD45-PE-Cy7, CD24-FITC, and Sca-1-PE. Total epithelial cells were collected and processed for

RNA to determine levels of *Hes1* gene expression by quantitative real-time reverse-transcription PCR.

For *in vitro* studies, cells were seeded in 3D Matrigel culture in 8-well chamber slides. After 12 hr, cultures were treated with 5 nM RO4929097 or vehicle (DMSO) for 4 days. Cells were fixed, permeabilized, and DAPI stained prior to quantification of orientations. RNA was collected using TRIzol for assessment of *Hes1* expression by quantitative real-time reverse-transcription PCR. See Extended Experimental Procedures for more information.

SUPPLEMENTAL INFORMATION

Supplemental Information includes Extended Experimental Procedures, nine figures, and two tables and can be found with this article online at <http://dx.doi.org/10.1016/j.celrep.2013.05.044>.

ACKNOWLEDGMENTS

We thank Elaine Fuchs (Howard Hughes Medical Institute and Rockefeller University) for the gift of *Krt14-mRFP* mice. The authors would like to thank Clare Isacke for her helpful comments on the manuscript. This study was funded by Breakthrough Breast Cancer. We acknowledge NHS funding to the NIHR Biomedical Research Centre. M.J.S. is supported by Cardiff University, Breast Cancer Campaign, and Cancer Research UK.

Received: March 21, 2012

Revised: April 16, 2013

Accepted: May 29, 2013

Published: June 27, 2013

REFERENCES

- Beleut, M., Rajaram, R.D., Caikovski, M., Ayyanan, A., Germano, D., Choi, Y., Schneider, P., and Briskin, C. (2010). Two distinct mechanisms underlie progesterone-induced proliferation in the mammary gland. *Proc. Natl. Acad. Sci. USA* **107**, 2989–2994.
- Betschinger, J., and Knoblich, J.A. (2004). Dare to be different: asymmetric cell division in *Drosophila*, *C. elegans* and vertebrates. *Curr. Biol.* **14**, R674–R685.
- Bibby, R.A., Tang, C., Faisal, A., Drosopoulos, K., Lubbe, S., Houlston, R., Bayliss, R., and Linardopoulos, S. (2009). A cancer-associated aurora A mutant is mislocalized and misregulated due to loss of interaction with TPX2. *J. Biol. Chem.* **284**, 33177–33184.
- Bird, A.W., and Hyman, A.A. (2008). Building a spindle of the correct length in human cells requires the interaction between TPX2 and Aurora A. *J. Cell Biol.* **182**, 289–300.
- Bischoff, J.R., Anderson, L., Zhu, Y., Mossie, K., Ng, L., Souza, B., Schryver, B., Flanagan, P., Clairvoyant, F., Ginther, C., et al. (1998). A homologue of *Drosophila* aurora kinase is oncogenic and amplified in human colorectal cancers. *EMBO J.* **17**, 3052–3065.
- Bissell, M.J., Rizki, A., and Mian, I.S. (2003). Tissue architecture: the ultimate regulator of breast epithelial function. *Curr. Opin. Cell Biol.* **15**, 753–762.
- Bouras, T., Pal, B., Vaillant, F., Harburg, G., Asselin-Labat, M.L., Oakes, S.R., Lindeman, G.J., and Visvader, J.E. (2008). Notch signaling regulates mammary stem cell function and luminal cell-fate commitment. *Cell Stem Cell* **3**, 429–441.
- Buono, K.D., Robinson, G.W., Martin, C., Shi, S., Stanley, P., Tanigaki, K., Honjo, T., and Hennighausen, L. (2006). The canonical Notch/RBP-J signaling pathway controls the balance of cell lineages in mammary epithelium during pregnancy. *Dev. Biol.* **293**, 565–580.
- Carroll, D.K., Carroll, J.S., Leong, C.O., Cheng, F., Brown, M., Mills, A.A., Brugge, J.S., and Ellisen, L.W. (2006). p63 regulates an adhesion programme and cell survival in epithelial cells. *Nat. Cell Biol.* **8**, 551–561.
- Cayouette, M., and Raff, M. (2002). Asymmetric segregation of Numb: a mechanism for neural specification from *Drosophila* to mammals. *Nat. Neurosci.* **5**, 1265–1269.
- Cumming, G., Fidler, F., and Vaux, D.L. (2007). Error bars in experimental biology. *J. Cell Biol.* **177**, 7–11.
- Da Silva, L., and Lakhani, S.R. (2010). Pathology of hereditary breast cancer. *Mod. Pathol.* **23**(Suppl 2), S46–S51.
- Fielding, A.B., Lim, S., Montgomery, K., Dobreva, I., and Dedhar, S. (2011). A critical role of integrin-linked kinase, ch-TOG and TACC3 in centrosome clustering in cancer cells. *Oncogene* **30**, 521–534.
- Giet, R., McLean, D., Descamps, S., Lee, M.J., Raff, J.W., Prigent, C., and Glover, D.M. (2002). *Drosophila* Aurora A kinase is required to localize D-TACC to centrosomes and to regulate astral microtubules. *J. Cell Biol.* **156**, 437–451.
- Harrison, H., Farnie, G., Howell, S.J., Rock, R.E., Stylianou, S., Brennan, K.R., Bundred, N.J., and Clarke, R.B. (2010). Regulation of breast cancer stem cell activity by signaling through the Notch4 receptor. *Cancer Res.* **70**, 709–718.
- Horvitz, H.R., and Herskowitz, I. (1992). Mechanisms of asymmetric cell division: two Bs or not two Bs, that is the question. *Cell* **68**, 237–255.
- Hutterer, A., Berdnik, D., Wirtz-Peitz, F., Zigman, M., Schleiffer, A., and Knoblich, J.A. (2006). Mitotic activation of the kinase Aurora-A requires its binding partner Bora. *Dev. Cell* **11**, 147–157.
- Kais, Z., Chiba, N., Ishioka, C., and Parvin, J.D. (2012). Functional differences among BRCA1 missense mutations in the control of centrosome duplication. *Oncogene* **31**, 799–804.
- Kasper, M., Jakob, V., Fiaschi, M., and Toftgård, R. (2009). Hedgehog signalling in breast cancer. *Carcinogenesis* **30**, 903–911.
- Kendrick, H., Regan, J.L., Magnay, F.A., Grigoriadis, A., Mitsopoulos, C., Zvelebil, M., and Smalley, M.J. (2008). Transcriptome analysis of mammary epithelial subpopulations identifies novel determinants of lineage commitment and cell fate. *BMC Genomics* **9**, 591.
- Lechler, T., and Fuchs, E. (2005). Asymmetric cell divisions promote stratification and differentiation of mammalian skin. *Nature* **437**, 275–280.
- Lee, C.Y., Andersen, R.O., Cabernard, C., Manning, L., Tran, K.D., Lanskey, M.J., Bashirullah, A., and Doe, C.Q. (2006). *Drosophila* Aurora-A kinase inhibits neuroblast self-renewal by regulating aPKC/Numb cortical polarity and spindle orientation. *Genes Dev.* **20**, 3464–3474.
- Lee, C.W., Simin, K., Liu, Q., Plescia, J., Guha, M., Khan, A., Hsieh, C.C., and Altieri, D.C. (2008). A functional Notch-survivin gene signature in basal breast cancer. *Breast Cancer Res.* **10**, R97.
- Leontovich, A.A., Salisbury, J.L., Veroux, M., Tallarita, T., Billadeau, D., McCubrey, J., Ingle, J., Galanis, E., and D'Assoro, A.B. (2013). Inhibition of Cdk2 activity decreases Aurora-A kinase centrosomal localization and prevents centrosome amplification in breast cancer cells. *Oncol. Rep.* **29**, 1785–1788.
- Leung, C.T., and Brugge, J.S. (2012). Outgrowth of single oncogene-expressing cells from suppressive epithelial environments. *Nature* **482**, 410–413.
- Li, L., and Xie, T. (2005). Stem cell niche: structure and function. *Annu. Rev. Cell Dev. Biol.* **21**, 605–631.
- Ma, N., Titus, J., Gable, A., Ross, J.L., and Wadsworth, P. (2011). TPX2 regulates the localization and activity of Eg5 in the mammalian mitotic spindle. *J. Cell Biol.* **195**, 87–98.
- McCaffrey, L.M., and Macara, I.G. (2011). Epithelial organization, cell polarity and tumorigenesis. *Trends Cell Biol.* **21**, 727–735.
- Parr, C., Watkins, G., and Jiang, W.G. (2004). The possible correlation of Notch-1 and Notch-2 with clinical outcome and tumour clinicopathological parameters in human breast cancer. *Int. J. Mol. Med.* **14**, 779–786.
- Reedijk, M., Odoricic, S., Chang, L., Zhang, H., Miller, N., McCready, D.R., Lockwood, G., and Egan, S.E. (2005). High-level coexpression of JAG1 and NOTCH1 is observed in human breast cancer and is associated with poor overall survival. *Cancer Res.* **65**, 8530–8537.
- Regan, J.L., Kendrick, H., Magnay, F.A., Vafaizadeh, V., Groner, B., and Smalley, M.J. (2012). c-Kit is required for growth and survival of the cells of origin of Brca1-mutation-associated breast cancer. *Oncogene* **31**, 869–883.

- Richert, M.M., Schwertfeger, K.L., Ryder, J.W., and Anderson, S.M. (2000). An atlas of mouse mammary gland development. *J. Mammary Gland Biol. Neoplasia* 5, 227–241.
- Romano, R.A., Ortt, K., Birkaya, B., Smalley, K., and Sinha, S. (2009). An active role of the DeltaN isoform of p63 in regulating basal keratin genes K5 and K14 and directing epidermal cell fate. *PLoS One* 4, e5623.
- Shackleton, M., Vaillant, F., Simpson, K.J., Stingl, J., Smyth, G.K., Asselin-Labat, M.L., Wu, L., Lindeman, G.J., and Visvader, J.E. (2006). Generation of a functional mammary gland from a single stem cell. *Nature* 439, 84–88.
- Siller, K.H., and Doe, C.Q. (2009). Spindle orientation during asymmetric cell division. *Nat. Cell Biol.* 11, 365–374.
- Sleeman, K.E., Kendrick, H., Robertson, D., Isacke, C.M., Ashworth, A., and Smalley, M.J. (2007). Dissociation of estrogen receptor expression and in vivo stem cell activity in the mammary gland. *J. Cell Biol.* 176, 19–26.
- Srinivasan, K., Strickland, P., Valdes, A., Shin, G.C., and Hinck, L. (2003). Netrin-1/neogenin interaction stabilizes multipotent progenitor cap cells during mammary gland morphogenesis. *Dev. Cell* 4, 371–382.
- Stingl, J., Eirew, P., Ricketson, I., Shackleton, M., Vaillant, F., Choi, D., Li, H.I., and Eaves, C.J. (2006). Purification and unique properties of mammary epithelial stem cells. *Nature* 439, 993–997.
- Taddei, I., Deugnier, M.A., Faraldo, M.M., Petit, V., Bouvard, D., Medina, D., Fässler, R., Thiery, J.P., and Glukhova, M.A. (2008). Beta1 integrin deletion from the basal compartment of the mammary epithelium affects stem cells. *Nat. Cell Biol.* 10, 716–722.
- Torchia, E.C., Chen, Y., Sheng, H., Katayama, H., Fitzpatrick, J., Brinkley, W.R., Caulin, C., Sen, S., and Roop, D.R. (2009). A genetic variant of Aurora kinase A promotes genomic instability leading to highly malignant skin tumors. *Cancer Res.* 69, 7207–7215.
- Van Keymeulen, A., Rocha, A.S., Ousset, M., Beck, B., Bouvencourt, G., Rock, J., Sharma, N., Dekoninck, S., and Blanpain, C. (2011). Distinct stem cells contribute to mammary gland development and maintenance. *Nature* 479, 189–193.
- van Amerongen, R., Bowman, A.N., and Nusse, R. (2012). Developmental stage and time dictate the fate of Wnt/β-catenin-responsive stem cells in the mammary gland. *Cell Stem Cell* 11, 387–400.
- Visbal, A.P., and Lewis, M.T. (2010). Hedgehog signaling in the normal and neoplastic mammary gland. *Curr. Drug Targets* 11, 1103–1111.
- Williams, J.M., and Daniel, C.W. (1983). Mammary ductal elongation: differentiation of myoepithelium and basal lamina during branching morphogenesis. *Dev. Biol.* 97, 274–290.
- Yamamoto, Y., Ibusuki, M., Nakano, M., Kawasoe, T., Hiki, R., and Iwase, H. (2009). Clinical significance of basal-like subtype in triple-negative breast cancer. *Breast Cancer* 16, 260–267.
- Zhang, L., Stokes, N., Polak, L., and Fuchs, E. (2011). Specific microRNAs are preferentially expressed by skin stem cells to balance self-renewal and early lineage commitment. *Cell Stem Cell* 8, 294–308.
- Zhou, H., Kuang, J., Zhong, L., Kuo, W.L., Gray, J.W., Sahin, A., Brinkley, B.R., and Sen, S. (1998). Tumour amplified kinase STK15/BTAK induces centrosome amplification, aneuploidy and transformation. *Nat. Genet.* 20, 189–193.